GEOLOGICA CARPATHICA, APRIL 2009, 60, 2, 107–119 doi: 10.2478/v10096-009-0007-2

Low pressure migmatites from the Sanandaj-Sirjan Metamorphic Belt in the Hamedan region (Iran)

ALI A. SEPAHI*, SEYEDEH R. JAFARI and SARA MANI-KASHANI

Department of Geology, Bu-Ali Sina University, Hamedan, Iran; *sepahi@basu.ac.ir

(Manuscript received February 23, 2008; accepted in revised form October 23, 2008)

Abstract: Migmatites with evidence for low pressure metamorphism and partial melting occur adjacent to the Alvand Plutonic Complex in the Hamedan region of Iran. They show stromatic, schollen, diktyonitic and massive structure. Sillimanite/andalusite/(kyanite)-garnet- and cordierite-K-feldspar-andalusite-spinel-bearing migmatites are the most common rock types. Some of the granitic intrusions contain xenocrysts which resemble the porphyroblasts of nearby migmatites (e.g. sillimanite, andalusite, cordierite and garnet). Although migmatitic rocks of the region are located near the granitic intrusions, the degree of partial melting is not related to intrusions and is irregular. It appears that partial melting and migmatization pre-date the intrusion of major granitic bodies in the region. Leucosomes in stromatic migmatites are commonly parallel to bedding planes and are mostly formed by metamorphic segregation and/or *in situ* partial melting (showing mafic selvedges, pinch and swell structures). The melt fraction and migmatite type depend on the chemical composition of parent rocks and the distribution of high strain zones. The formation of thin leucosomes in the stromatic migmatites was controlled by short-range melt movement along the grain boundaries. Melt-rich layers are constrained by pre-existing compositional layering and foliation. Peak metamorphic conditions of ~650 °C and ~300 MPa are consistent with the observed mineral assemblages and the presence of melt in the investigated migmatites.

Key words: Iran, Sanandaj-Sirjan, Hamedan, anatexis, granite, migmatite.

Introduction

Migmatites can be generated by four major processes: a) injection of externally derived magmas (Sederholm 1913), b) partial melting (Sederholm 1913; Holmquist 1921; Mehnert 1968), c) metasomatism (Misch 1968) and d) metamorphic differentiation (Robin 1979; Ashworth & McLellan 1985). Each of these processes can be responsible for generating migmatitic rocks in the particular metamorphic belt.

In the last fifty years, the migmatites and their relationships to granitic intrusions have been investigated (e.g. Mehnert 1968; Ashworth 1985; Brown 1994; Sawyer 1996, 2001). Petrogenesis of the layer-parallel leucosomes and the importance of stress and deformation for the generation of migmatitic rocks were considered (e.g. Sawyer & Barnez 1988, and Marchildon & Brown 2002). Layer-parallel leucosomes can be formed by sub-solidus processes due to mobilization of quartz and feldspar by stress-induced mass-transfer of mobile elements (Sawyer & Barnez 1988) or by anatectic processes (Marchildon & Brown 2002, 2003). In this paper, we present evidence from the Hamedan region in Iran that layer-parallel leucosomes may have originated by both sub-solidus and anatectic processes during progressive high-grade metamorphism. In the outcrops, the various stages of migmatization, from initial sedimentary layers to sub-solidus leucosomes and finally to anatectic leucosomes can be observed.

Field, petrographic and geochemical data on magmatism and metamorphism in the Hamedan region have been presented in some recent works (e.g. Irani 1993; Hadipour 1994; Sadeghian 1994; Torkian 1995; Baharifar 1997, 2004; Sepahi 1999; Sepahi et al. 2004); however, the petrogenesis of migmatites has not been considered yet. In this paper, we provide new data pertaining to the petrogenesis of migmatites (especially of stromatic migmatites) near to the Alvand Plutonic Complex in the Hamedan region.

Geological setting

The study area is a part of the so-called Sanandaj-Sirjan Zone or Zagros Imbricate Zone of the Zagros Orogen (according to Alavi 1994, 2004). This zone comprises a metamorphic belt of low- to high-grade regional and contact metamorphic rocks that have been intruded by mafic, intermediate and felsic plutonic bodies (Fig. 1). Major metamorphic and magmatic events of the Sanandaj-Sirjan Metamorphic Belt (SSMB) occurred during the Mesozoic Era (e.g. Baharifar 1997, 2004; Sepahi 1999; Rashidnejad-Omran et al. 2002; Sheikholeslami et al. 2003; Sepahi et al. 2004; Ahmadi-Khalaji et al. 2007). Major granitic plutons of the SSMB have been atributed to the Mesozoic-Tertiary magmatism (~200 to ~40 Ma; e.g. Valizadeh & Cantagrel 1975; Masoudi 1997; Baharifar 2004; Ahmadi-Khalaji et al. 2007; Arvin et al. 2007). These events have been related to the subduction of the Neo-Tethys and later collisional events (e.g. Baharifar 1997, 2004; Sepahi 1999 and Sepahi et al. 2004).

Field relations and petrography of the major plutonic and metamorphic rocks

In the Hamedan region, low- to high-grade, regional and contact metamorphic rocks occur adjacent to plutonic bodies (Fig. 2). Metapelitic rocks are the most abundant, compris-

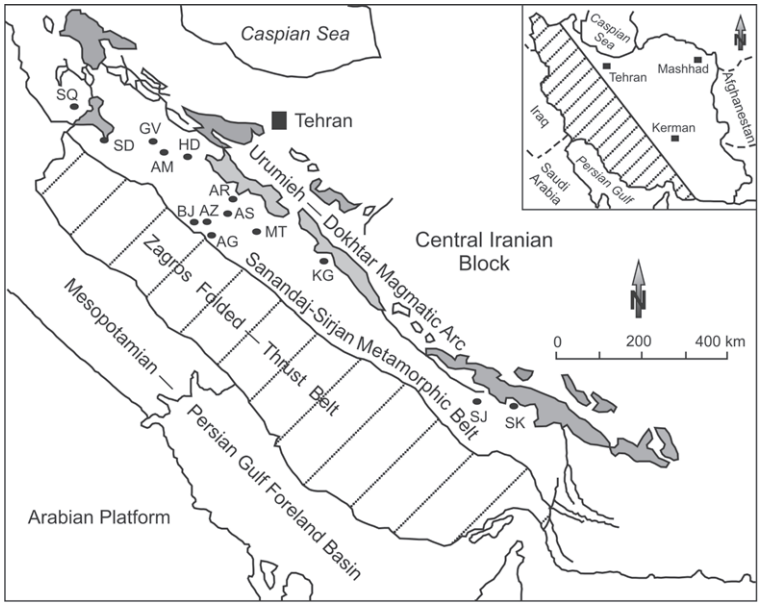

Fig. 1. Distribution of major plutonic bodies in the Sanandaj-Sirjan Metamorphic Belt, Zagros Orogen, Iran (tectonic units after Alavi 1994, 2004 and Mohajjel & Fergusson 2003; modified after Moazzen et al. 2004 and Sepahi & Athari 2006). **SQ** — Saqqez, **SD** — Sanandaj, **GH** — Ghorveh, **AM** — Almogholagh, **HD** — Hamedan (Alvand), **AR** — Arak, **AS** — Astaneh, **BJ** — Boroujerd, **AG** — Aligudarz, **AZ** — Azna, **MT** — Muteh, **KG** — Kolah-Ghazi, **SJ** — Sirjan, **SK** — Siah Kouh.

ing slates, phyllites, mica-schists, garnet-schists, garnet-andalusite-(±sillimanite/±kyanite)-schists, garnet-staurolite-schists and garnet-sillimanite-(±kyanite)-schists. They are inter-layered with minor metabasic rocks (amphibole-bearing schists and amphibolites), metacarbonates, and calc-silicate rocks. Near the Alvand Plutonic Complex, contact cordierite (Crd_2)-K-feldspar-(±andalusite, fibrous sillimanite)-hornfelses, garnet-staurolite (±kyanite) hornfelses, and in some places garnet-sillimanite-(±andalusite/±kyanite)-schists/migmatites with inter-layers of cordierite (Crd_1)-K-feldspar-andalusite-spinel-migmatites occur. Mineral abbreviations are used according to Kretz (1983).

In the eastern aureole of the Alvand Plutonic Complex, a suite of migmatitic rocks occur, which were first reported by Sepahi (1999). The contact of migmatites with nearby granitic bodies is usually sharp. Despite high-grade metamorphism, some bedding planes can be traced in the migmatitic rocks.

Two migmatite types are present, namely Al_2SiO_5-bearing and cordierite-(±andalusite)-bearing migmatites (Fig. 3a–b). Several structural varieties from stromatic to schollen, diktyonitic, nebulitic and massive can be seen in many localities (Fig. 3c–e). The progressive stages of partial melting can be observed in the outcrops (Fig. 3f–h). Metatexites show stromatic fabric with leucosomes commonly concordant to bedding planes, except in high strain zones, such as faults and shear zones. The foliation-parallel leucosomes are usually 5–20 mm thick. The distribution of most of the leucosomes is controlled by the spatial distribution of pre-existing compositional layering and foliation (Fig. 3i). Some boudin-like structures into which leucocratic material has segregated are developed in the inter-boudin partitions (Fig. 3j). Melts have also collected into some small shear zones forming the discordant leucosomes (Fig. 3k).

Aplitic-pegmatitic dykes are widespread in the migmatitic zone and appear to be late to post-anatectic features. They contain large amounts of tourmaline. Tourmaline also occurs in the metamorphic rocks near the dykes. In the field, retrograde reactions are visible in the migmatites/schists adjacent to the aplitic-pegmatitic dykes. The formation of muscovite and a second generation of staurolite (St_2), at the expense of andalusite/sillimanite porphyroblasts (Fig. 4), is a common feature near the dykes.

Except for a narrow zone (nearly 25 km long and up to 5 km wide) in which migmatitic rocks are in contact with intrusive bodies (i.e. granites), hornfelses with typical fine-grained granoblastic (hornfelsic) texture, particularly cordierite-hornfelses occur around intrusive bodies. Minor injection complex (migmatitic hornfelses) occurs at the contacts with granites (up to 50 meters from the contact zone). Migmatitic hornfelses are distinguished from the regional migmatites and migmatitic schists by their position close to the plutons, mineral assemblages and textures. Regionally metamorphosed schists/migmatites have schistose (porphyro-lepidoblastic) texture containing large porphyroblasts of sillimanite/andalusite (up to 20 cm), but hornfelses and contact migmatites (injection complex) have a massive structure and granoblastic texture without prismatic sillimanite (Fig. 5). In the injection complex, some of the leucocratic veins can be observed adjacent to the plutonic bodies. In contrast to injection migmatites, regional migmatites show various structures and occur over a wider area (especially to the south of Simin village, south of Hamedan city (sillimanite+K-feldspar+Crd_1 zone on Fig. 2)).

Plutonic rocks

The Alvand Plutonic Complex (Fig. 2) is one of the major plutonic complexes in the SSMB. It includes: 1) gabbro-diorite-tonalite (GDT) association, 2) granite-granodiorite porphyric rocks and 3) leucocratic granitoids. The GDT association consists of olivine gabbro, gabbro, gabbronorite, diorite, and tonalite, which were metamorphosed by the intrusion of younger granitic bodies. The monzogranite-granodiorites (G_2) contain feldspars (plagioclase, K-feldspar and minor microcline), quartz and biotite (rarely muscovite) without any hornblende. Xenocrysts of andalusite, sillimanite, garnet and cordierite are common in these rocks. Leucocratic granitoids (G_3) comprise leucotonalites, leucogranodiorites and leucogranites, forming small post-tectonic intrusions (Sepahi 1999).

In some of the granitic rocks, metamorphic (restitic) xenocrysts of garnet, andalusite/sillimanite and cordierite are widespread (Fig. 6a–c). These minerals were probably generated during the mechanical dispersion of restitic enclaves or xenoliths of schists and migmatites. Xenocrystic andalusite crystals show reaction microtextures, such as replacement of an-

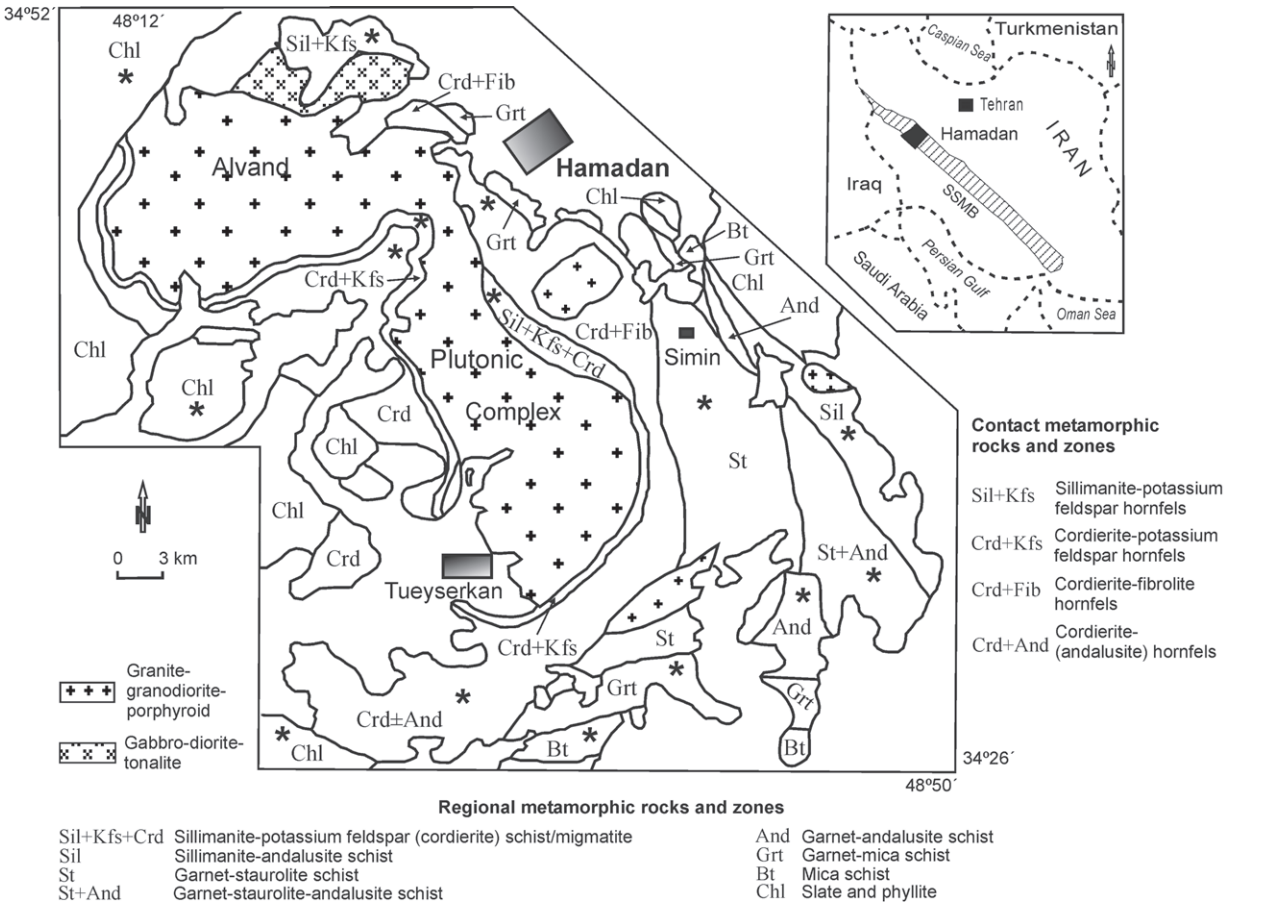

Fig. 2. Simplified geological map of the Hamedan region in the Sanandaj-Sirjan Metamorphic Belt showing the Alvand Plutonic Complex and major metamorphic zones of the region. * = the locations of sampling.

dalusite by sillimanite (Fig. 6d). The reaction between the andalusite/sillimanite xenocrysts and their granitic and dioritic host rocks indicates that andalusite/sillimanite has not crystallized from the granitic/dioritic melt (magma). Therefore, they came from the disaggregated country rocks during the ascent and emplacement of the plutons. In the classification scheme of Clarke et al. (2005), the andalusite xenocrysts of the Alvand Plutonic Complex are metamorphic. Also, garnets in the porphyritic granites are metamorphic xenocrysts (Sepahi 1999). Some garnet-bearing aplites-pegmatites occur, too. The garnet composition in these rocks is Mn-rich almandine.

Regional metamorphic rocks

The low P/high T (LP/HT) metamorphism of the region is characterized by the development of chlorite, biotite, garnet, andalusite, staurolite (St_1), sillimanite and sillimanite-K-feldspar (± cordierite) zones. The metamorphic zones have irregular outcrop patterns due to intense deformation related to the thrusting in the region that occurred after regional metamorphism. In particular, staurolite (St_1) and sillimanite zones are bounded by faults. The metamorphic rocks within the regional metamorphic zones are as follows:

Low-grade rocks (chlorite zone): The lowest-grade rocks of this zone are slates and phyllites, inter-layered with carbonate rocks and quartzites. Slates contain quartz, sericite, chlorite, graphite, iron oxides and pyrite. Phyllites contain quartz, chlorite, muscovite, plagioclase, graphite, ± biotite, ± garnet, as well as accessory calcite, tourmaline and iron oxides. This zone is the most widespread zone in the Sanandaj-Sirjan Metamorphic Belt as a whole (Fig. 2).

Mica ± garnet schists (biotite and garnet zones): The typical rocks of this zone are mica-schists showing lepido-porphyroblastic texture. These rocks contain quartz, biotite, garnet, muscovite, and chlorite, with accessory plagioclase, graphite, tourmaline, apatite, calcite and iron oxides. Garnets are typically almandine-rich (Alm > 60; Sepahi et al. 2004), but they have a considerable amounts of MnO and CaO according to their chemical compositions (see also section 5). In the AFM diagram (Fig. 7a) typical mineral assemblage of this zone is shown.

Andalusite-bearing schists (chiastolite zone): Andalusite-bearing rocks are medium- to coarse-grained, with porphyroblasts of garnet (up to 1 cm in diameter), and andalusite crystals (up to 20 cm in length; Fig. 8a). The common minerals are quartz, biotite, andalusite (chiastolite), garnet and muscovite. The minor minerals are staurolite, graphite, chlorite, plagioclase, fibrolite, tourmaline, ilmenite and rutile. An AFM diagram for the typical mineral assemblage of this zone is shown in Fig. 7b.

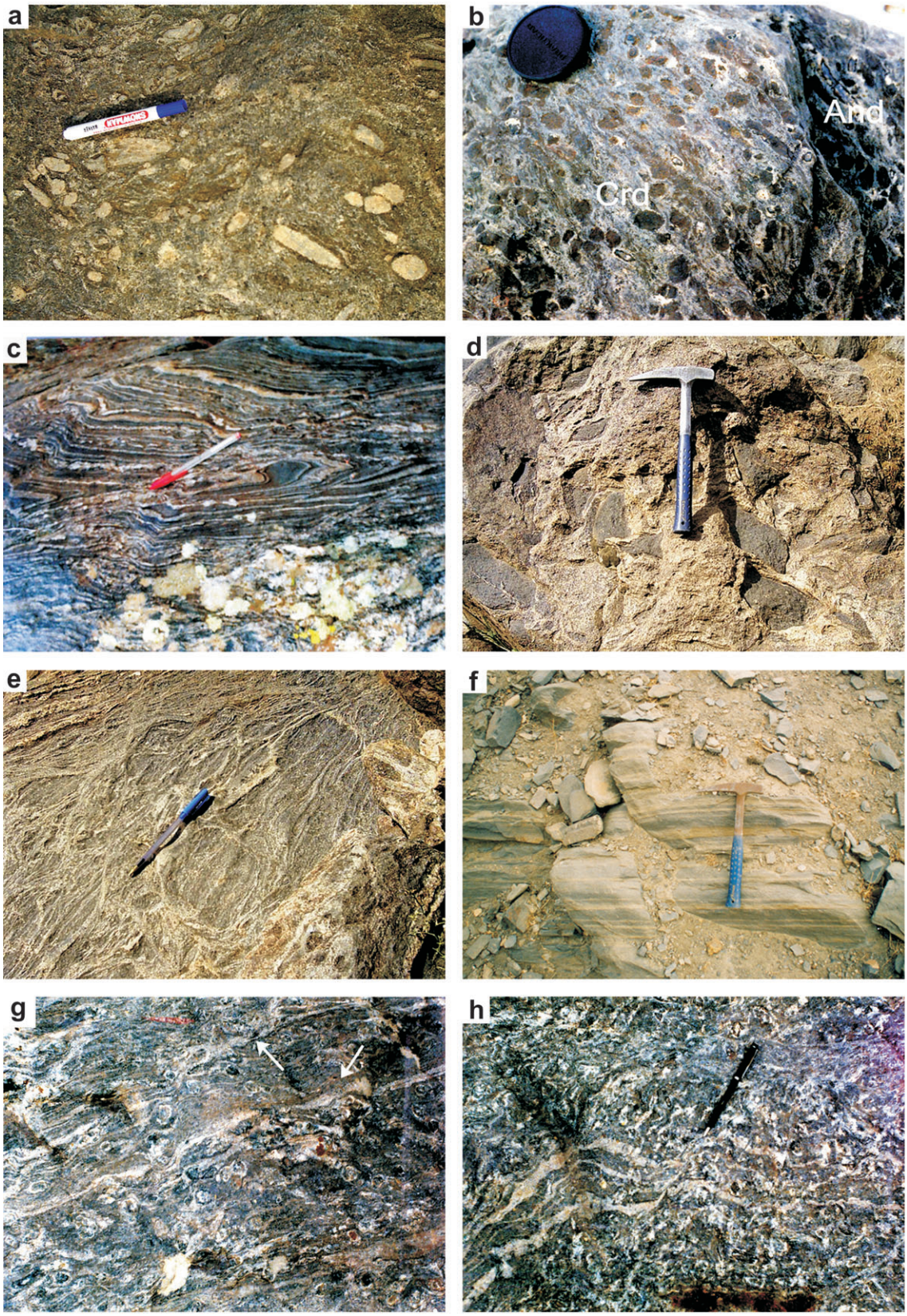

Fig. 3. Major mineralogical and structural types of migmatites in the Hamedan region: **a** — sillimanite-migmatite and **b** — cordierite-migmatite; **c** — stromatic structure; **d** — schollen structure; **e** — diktyonitic structure; **f–h** — progressive stages of partial melting in a pelitic-psammitic rock sequence from low degree (f — containing less melted and nearly undisturbed psammitic beds), to higher degree (g–h — containing disturbed and partially melted psammitic beds (shown by arrows); partial melting occurs around some of the Al_2SiO_5 porphyroblasts (g)).

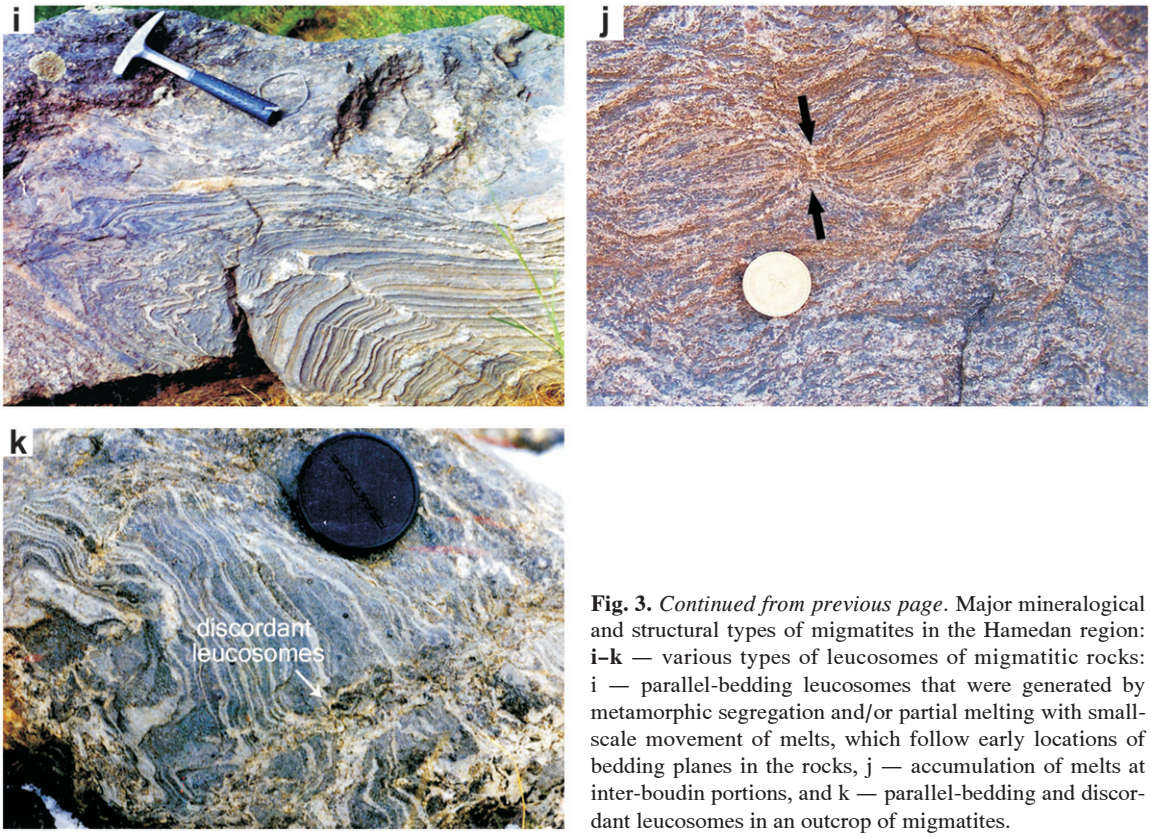

Fig. 3. *Continued from previous page*. Major mineralogical and structural types of migmatites in the Hamedan region: **i–k** — various types of leucosomes of migmatitic rocks: i — parallel-bedding leucosomes that were generated by metamorphic segregation and/or partial melting with small-scale movement of melts, which follow early locations of bedding planes in the rocks, j — accumulation of melts at inter-boudin portions, and k — parallel-bedding and discordant leucosomes in an outcrop of migmatites.

Fig. 4. Partial to complete replacement of sillimanite porphyroblasts by staurolite (± garnet) + muscovite + quartz in some high-grade schists/migmatites which are mostly indicated by arrows near them (for more explanations see text).

Fig. 5. Granitic veins cutting through massive cordierite-hornfelses producing limited injection complex (contact migmatites) near granitic bodies.

Staurolite-schists (staurolite zone): Staurolite-schists are composed of quartz, staurolite, garnet, biotite, muscovite, chlorite, plagioclase, graphite and tourmaline. The porphyroblasts of garnet are typically small (< 5 mm), but staurolite (staurolite 1) crystals are up to 15 cm long (Fig. 8b). The staurolite crystals are mostly Fe-rich ($X_{Fe} > 70$) and contain small amounts of Zn (Sepahi et al. 2004). The plagioclase has an intermediate composition and is unzoned or slightly zoned, from An_{36-29} in the cores to An_{29-32} in the rims. Chlorite is a retrograde mineral in these rocks. An AFM diagram for the typical mineral assemblage of this zone is shown in Fig. 7c.

Sillimanite-andalusite-schists (sillimanite zone): Sillimanite-andalusite-schists contain quartz, biotite, muscovite, plagioclase, and small garnet crystals (600–700 μm) with large (3–20 cm long) porphyroblasts of andalusite partially replaced by prismatic sillimanite (sillimanite also occurs in these rocks as fibrolite). Accessory minerals are graphite, tour-

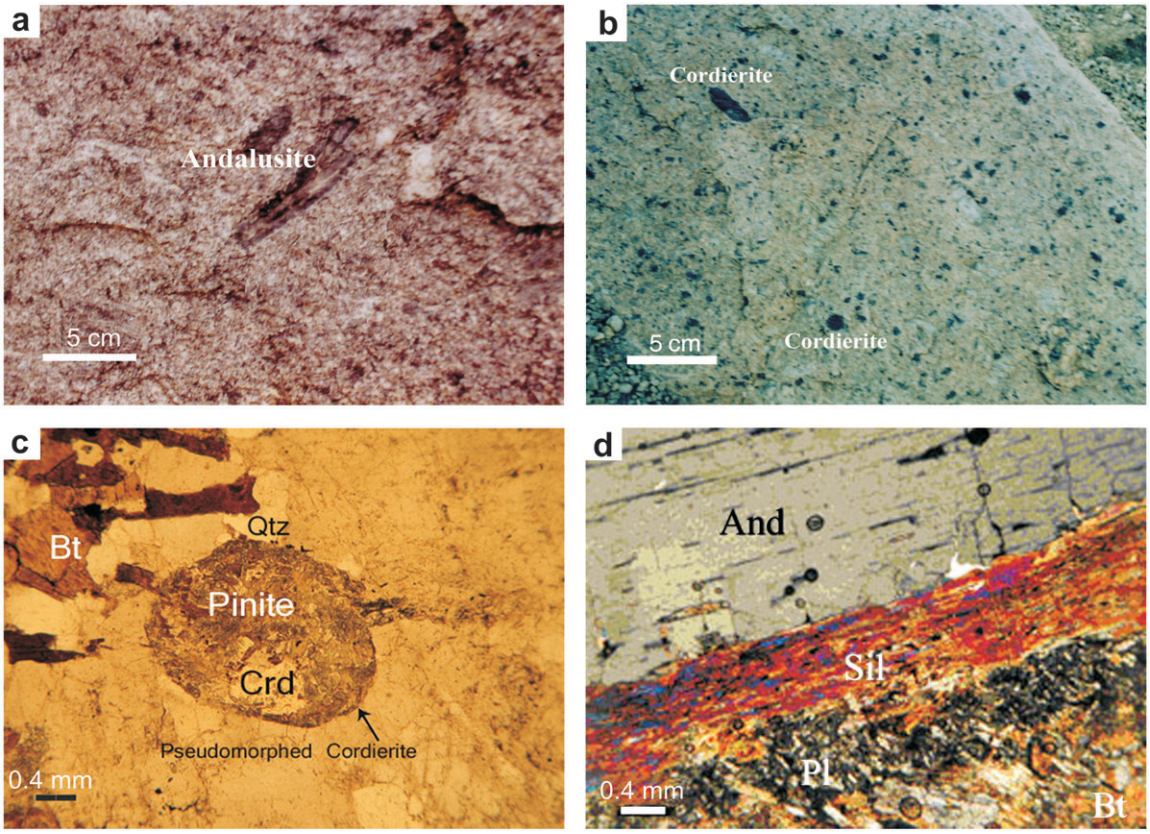

Fig. 6. a–c — Major types of enclaves and xenocrysts in the S-type granites of the APC: a — micaceous enclave and andalusite xenocryst, b — pinitized cordierite (outcrop photo), and c — pinitized cordierite (photomicrograph). **d** — Conversion of andalusite xenocryst to sillimanite in granites.

maline and ilmenite. An AFM diagram for the typical mineral assemblage of this zone is shown in Fig. 7d.

Kyanite-bearing schists and veins (not recognized in the map): Kyanite-schists occur at scattered localities within the other zones (especially in high-strain zones such as shear zones). In these rocks, kyanite frequently occurs as pseudomorphs after andalusite/sillimanite. The typical mineral assemblage of these rocks is biotite + plagioclase + quartz + kyanite ± garnet. The garnets of these rocks, are typically almandine-rich, elongate, and irregularly shaped. Kyanite-quartz veins cut through various lithologies especially in the metamorphic rocks close to granitic intrusions. Retrograde muscovite and chlorite are often present in these veins, as well as minor diaspore.

High-grade schists and migmatites (sillimanite-K-feldspar zone): The metamorphic rocks of this zone are composed of high-grade schists and migmatites adjacent to granitic bodies. Migmatites were observed within the 15 km of the ~120 km long contact zones in which sillimanite/andalusite schists/migmatites alternate with minor inter-layers of cordierite-bearing migmatites. The highest-grade schists in the regional metamorphic sequence contain sillimanite + quartz + biotite + muscovite + garnet + plagioclase + K-feldspar (pethitic K-feldspar) + ilmenite ± andalusite ± kyanite ± staurolite. With increasing metamorphic grade these schists continue into migmatitic rocks, in which mesosome mineralogy is similar to the mineral assemblages in the schists. These schists are cut by abundant granitic pegmatites and sillimanite-quartz veins. The inter-layers contain cordierite (Crd_1), perthitic K-feldspar, minor biotite, plagioclase, spinel and opaque minerals. In these rocks, symplectitic intergrowth of cordierite with spinel is visible around some andalusite porphyroblasts.

This zone is associated with partial melting and development of granitic leucosomes in migmatites. Plagioclase-rich (trondjhemitic) leucosomes are predominant, but some contain additional K-feldspar. Mesosomes of migmatites have porphyro-lepidoblastic texture and contain quartz, biotite, garnet and Al_2SiO_5 polymorphs, especially sillimanite (but also andalusite/kyanite) ± staurolite ± spinel ± cordierite(Crd_1) ± graphite. Leucosomes of migmatites have granoblastic texture and contain quartz, plagioclase (in some places K-feldspar) and muscovite (± garnet). Melanosomes are less developed and resemble the mesosomes with respect to their mineralogy and texture, except for greater amounts of mafic minerals and smaller amounts of felsic minerals.

Al_2SiO_5-bearing migmatites are the most common rocks in the migmatitic suite. Andalusite/sillimanite-bearing rocks are predominant, but some kyanite-bearing rocks also occur, especially in shear zones in which kyanite developed after andalusite/sillimanite porphyroblasts. Garnet crystals of millimeter to centimeter size (up to 2 cm) are common in these rocks. There are two prograde and retrograde assemblages in

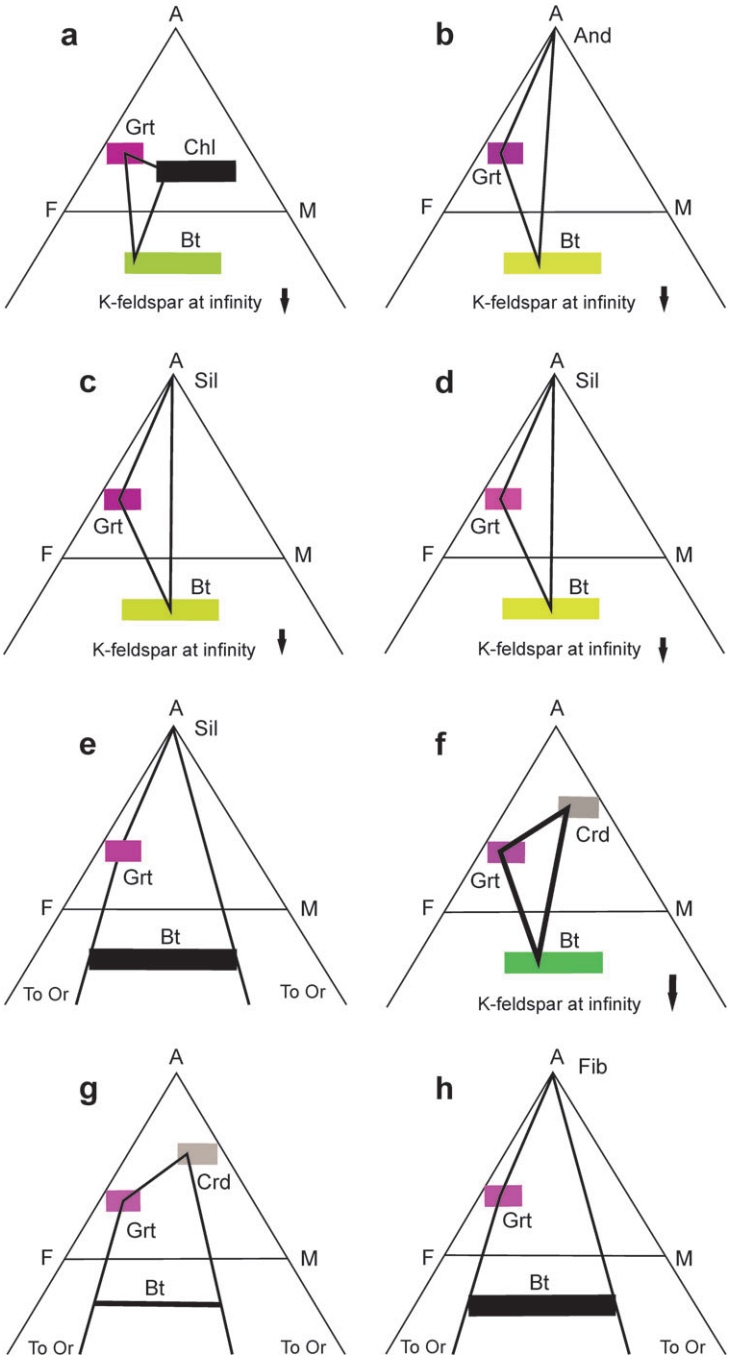

Fig. 7. AFM diagrams for typical mineral assemblages from various metamorphic zones. **a** — garnet zone, **b** — andalusite zone, **c** — staurolite zone, **d** — sillimanite zone, **e** — sillimanite-K-feldspar zone, **f** — cordierite(Crd_2)-(andalusite) zone, **g** — cordierite (Crd_2)-K-feldspar zone and **h** — fibrolitic sillimanite (Sil_2)-K-feldspar zone. Zones a–e are regional metamorphic zones and zones f–h are contact metamorphic zones. Quartz and muscovite (commonly retrograde) are roughly present in each zone.

Al_2SiO_5-bearing migmatitic rocks; a prograde (sillimanite/andalusite)-K-feldspar-biotite-(± garnet)-quartz assemblage (Fig. 7e) and a retrograde staurolite (St_2)-muscovite-(± garnet)-(± Ky) assemblage. Retrograde staurolite (St_2) occurs around and inside large porphyroblasts of Al_2SiO_5 minerals (especially sillimanite and in some places, andalusite/kyanite, Fig. 4). Cordierite-rich layers also occur in some parts of the migmatitic sequence. They are composed of quartz, biotite, cordierite (Crd_1), andalusite and K-feldspar, with minor spinel and plagioclase. Symplectite texture generated by cordierite-spinel intergrowth occurs on the rim of some andalusite porphyroblasts.

Contact metamorphic rocks

The protoliths of the contact metamorphic rocks are similar to those in the regional metamorphic sequence and include abundant metapelitic rocks. Spotted schists containing muscovite-staurolite-chlorite spots, which were formed due to intrusion of plutonic bodies, are common in 1–2 km far from the contact of plutonic bodies. The following reaction may be responsible for the appearance of these spots:

Biotite + Andalusite + Quartz + H_2O = Staurolite + Muscovite + Chlorite.

Rocks with hornfelsic texture, but showing primary regional metamorphic assemblages, such as deformed andalusite, and kyanite (Ky_1) are common in the contact aureole. In some of the kyanite-schists/hornfelses in the contact zone, two distinct generations of kyanite are observable. In these rocks, some of the kyanite crystals are deformed, but other kyanites are euhedral, randomly oriented and cross-cut the relict foliation. Sequential development of the Al_2SiO_5 polymorphs during poly-metamorphic events is observable in some of the hornfelsic rocks. Andalusite-($kyanite_1$)-fibrolite sequential development is predominant, but sequential development of andalusite-($kyanite_1$)-fibrolite-$kyanite_2$ is also common in the hornfelsic rocks near to the quartz-kyanite veins. Texturally-late cordierite (Crd_2) also occurs in some of the hornfelsed schists. The highest-grade hornfelsic rocks of the region are distinguished by development of $cordierite_2$, K-feldspar and fibrolitic sillimanite (Sil_2) adjacent to intrusive bodies. Rocks in the inner contact zone include cordierite ± andalusite ± garnet-hornfels (cordierite-andalusite zone), cordierite-K-feldspar ± garnet-hornfels (cordierite-K-feldspar zone), and sillimanite-K-feldspar ± garnet-hornfels.

Two metamorphic zones are widespread around plutonic bodies: contact cordierite (Crd_2) ± fibrous sillimanite (Sil_2) ± andalusite and cordierite-K-feldspar zones. In addition, a narrow sillimanite (fibrolite = Sil_2)-K-feldspar zone is common around the gabbro-dioritic intrusive bodies (Fig. 2).

Cordierite-(andalusite) zone: The major rock types in this zone are cordierite-(andalusite)-hornfelses. Cordierite-(andalusite)-hornfelses occur all around the Alvand Plutonic Complex, except for some localities where sillimanite-hornfelses occur near the gabbroic rocks and also where regional

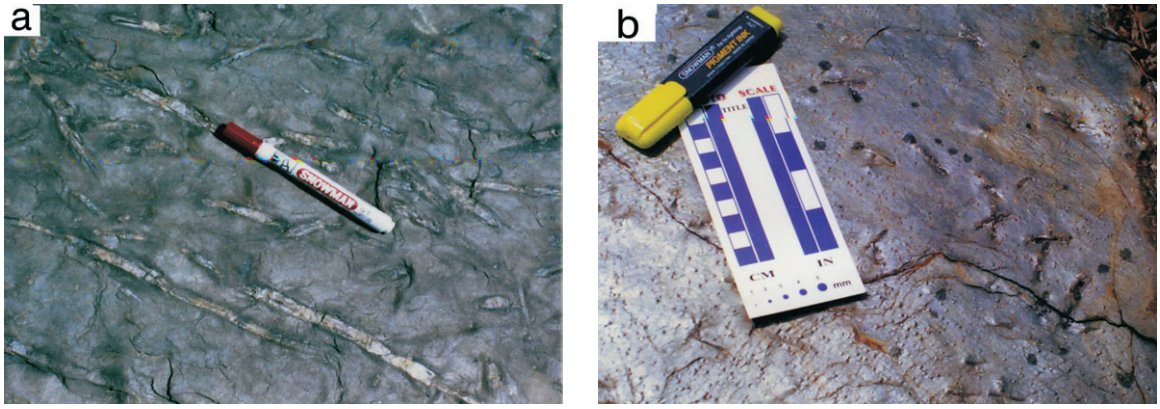

Fig. 8. Outcrops of two major regional metamorphic rock units of the region: (**a**) andalusite- and (**b**) staurolite-schists.

migmatites occur at a sharp contact with plutons. The typical mineral assemblage of this zone is quartz + biotite + contact cordierite (Crd_2) ± garnet ± fibrolite + plagioclase + opaque minerals ± (relict andalusite). An AFM diagram for the typical mineral assemblage of this zone is shown in Fig. 7f.

Cordierite-K-feldspar zone: Adjacent to the plutonic rocks (contact zone) there is a narrow zone of cordierite-K-feldspar. This metamorphic zone is common around the granitic part of the Alvand Plutonic Complex and is characterized by coexisting cordierite and perthitic K-feldspar. The typical mineral assemblage of these rocks is quartz + contact cordierite (Crd_2) + K-feldspar + biotite + minor plagioclase ± garnet and opaque minerals. An AFM diagram for the typical mineral assemblage of this zone is shown in Fig. 7g.

Fibrolite-K-feldspar zone: A narrow fibrolite-K-feldspar zone can be observed around gabbro-dioritic bodies, in some places. In these rocks, some of the garnet crystals are relicts from the previous regional metamorphic event, which are partly converted to fibrolitic sillimanite and biotite. In the leucocratic veins which cross cut through these rocks, preferred crystallization of some other garnet crystals also occurs alongside the veins. Therefore, two regional and contact metamorphic assemblages can be distinguished in these rocks: 1 — an older regional metamorphic assemblage of quartz-$biotite_1$-$garnet_1$-andalusite, 2 — a younger contact metamorphic assemblage of quartz-fibrolite-$biotite_2$-(±$garnet_2$, ±K-feldspar, ±muscovite). An AFM diagram for the typical mineral assemblage (assemblage 2) of this zone is shown in Fig. 7h.

Mineral chemistry

The major metamorphic rocks (and protoliths of the migmatites) include semipelitic and psammitic rocks but pelitic lithologies are rather widespread (Table 1, Fig. 9); they are inter-layered with some metabasic rocks. The chemical composition of metamorphic minerals (chlorite, biotite, muscovite, garnet, andalusite, kyanite, sillimanite, staurolite, cordierite and feldspars) have been described in some recent publications (e.g. Sepahi et al. 2004 and Baharifar 2004). The mineral compositions presented in this paper, were obtained using a JEOL JXA-8900 electron microprobe at the University of Minnesota, USA. Operating conditions for quantitive analysis (WSD) were 15 kV accelerating voltage, 15–25 nA beam current and a range of 5–20 μm beam diameters.

The chemical compositions of minerals in the metamorphic and migmatitic rocks are presented in the Tables 2–3. The range of XMg in biotite in the metamorphic rocks is between 0.3 and 0.6, but biotite in the higher-grade rocks has larger XMg in contrast to lower-grade ones (Table 2). In the muscovite of migmatitic rocks (samples MM1–MM3 in Table 3), which come from the sillimanite-K-feldspar zone (Fig. 2), the Na/(Na+K) ratios are mostly lower than 0.3. These are also lower than the ratios for mica-schists (samples MS1–MS5 in Table 3), from the biotite zone (Fig. 2) and hornfelses (samples MH1–MH2 in Table 3), from the cordierite zone. Staurolite is commonly Fe-rich (Sepahi et al. 2004). Garnet is mostly almandine-rich both in low-grade and medium–high-grade rocks, with considerable amounts of MnO and CaO (Sepahi et al. 2004). It is worth noting that the stability of garnet in metapelites expands to the lower temperature and pressure with the addition of Mn, hence garnet appears as a stable phase at low pressures (Mahar et al. 1997). Plagioclase in the mesosome of migmatites (An_{44} at core to An_{41} at rim) is more calcic than in the surrounding lower-grade metamorphic rocks (e.g. in nearby staurolite schists; An_{39} at core to An_{29} at rim).

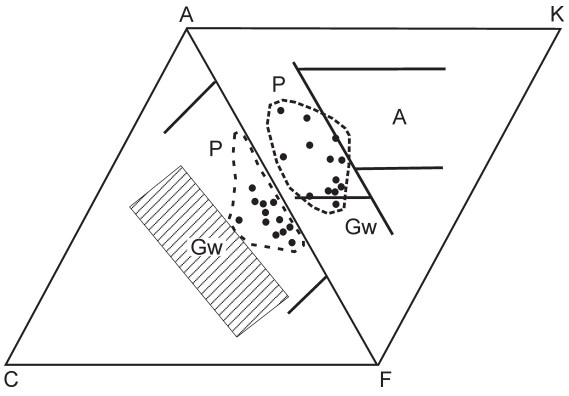

Fig. 9. A simplified ACFK diagram (modified after Winkler 1976) representing chemical compositions of the metamorphic rocks of the Hamedan region (circled field). **P** — Pelitic rocks, **A** — Arkose, **Gw** — Greywackes.

Table 1: Representative chemical analyses for some of the metamorphic rocks of the region (data from Baharifar 1997 and Sepahi 1999). Four samples are hornfelses (marked *) and the other ones are regional metamorphic rocks.

Samples/Oxides (wt. %)	Zg-Msh	Zg-ash	Ph-Meh	Gj-Absd$_5$*	Gj-Absd$_3$*	Ph-Hs	Sch-Kh
SiO_2	59.94	60.00	60.67	61.56	64.26	67.96	61.34
TiO_2	0.90	0.93	1.04	0.95	0.92	0.80	0.98
Al_2O_3	18.14	20.14	20.63	20.00	17.77	15.93	19.08
Fe_2O_3	7.51	10.40	8.91	7.30	7.44	1.34	1.49
FeO	–	–	–	–	–	3.87	5.14
MnO	0.11	0.14	0.13	0.09	0.13	–	–
MgO	2.76	2.35	2.72	2.24	2.52	1.71	2.22
CaO	3.02	0.52	0.60	0.56	0.42	0.70	0.74
K_2O	4.70	4.72	3.81	5.18	4.63	3.39	4.30
Na_2O	2.33	0.30	0.82	1.54	1.42	0.71	0.75
P_2O_5	0.19	0.25	0.09	0.18	0.16	–	–
Total	99.60	99.75	99.42	99.60	99.67	96.41	96.04

Samples/Oxides (wt. %)	Hfs-Jh*	Sch-Zg	Hfs-Dn*	Sch-Nj	Sch-Az	Sch-Chp	Sch-Ab
SiO_2	64.98	57.61	63.52	60.53	65.79	60.79	65.53
TiO_2	0.79	0.83	0.80	0.84	0.75	0.70	0.80
Al_2O_3	17.66	20.44	18.82	19.35	17.05	23.92	18.16
Fe_2O_3	0.03	3.48	0.48	1.57	2.44	2.34	0.58
FeO	6.56	3.93	6.00	4.66	3.13	3.35	5.39
MgO	3.15	2.48	2.29	3.22	2.04	1.89	3.14
CaO	0.75	0.83	0.72	3.41	1.01	0.71	0.58
K_2O	3.41	5.33	3.98	3.54	3.16	3.65	3.22
Na_2O	3.41	1.34	1.80	3.20	1.41	0.54	1.83
Total	100.74	96.27	98.41	100.32	96.78	97.89	99.03

Table 2: Electron microprobe representative analyses (wt. %) of biotite in staurolite-schists (BS_1–BS_4), cordierite-hornfelses (BH_1-BH_4) and in melanosome of migmatites (BM_1-BM_6) of the region.

Samples	BS_1	BS_2	BS_3	BS_4	BH_1	BH_2	BH_3	BH_4	BM_1	BM_2	BM_3	BM_4	BM_5	BM_6
SiO_2 (wt. %)	33.41	34.48	34.30	34.80	35.94	35.11	35.39	35.79	35.62	35.49	35.28	35.32	35.50	34.94
TiO_2	1. 53	1.81	1.68	1.88	1.68	1.63	1.50	1.58	1.73	1.69	1.68	1.71	1.79	1.68
Al_2O_3	20.25	20.53	20.14	20.51	20.69	19.67	20.02	19.91	20.20	20.24	20.15	19.90	20.25	19.66
FeO	20.91	20.47	20.37	20.40	20.03	21.03	20.91	20.77	20.31	19.73	19.31	20.03	19.84	20.61
MnO	0. 32	0.32	0.31	0.28	0.06	0.04	0.08	0.08	0.04	0.01	0.04	0.03	0.03	0.07
MgO	9. 92	9.85	10.08	9.83	9.29	9.54	9.68	9.91	9.91	9.92	9.85	9.92	9.84	9.71
CaO	0. 28	0.18	0.17	0.16	0.07	0.02	0.02	0.06	0.04	0.05	0.33	0.09	0.00	0.04
Na_2O	0. 21	0.43	0.30	0.36	0.27	0.28	0.27	0.26	0.13	0.19	0.05	0.19	0.23	0.20
K_2O	7. 33	8.82	8.89	9.10	8.05	9.25	8.98	8.88	8.79	8.73	6.99	8.62	8.90	8.63
Total	94.16	96.88	96.23	97.33	96.08	96.58	96.85	97.24	96.76	96.04	93.68	95.81	96.37	95.51
Number of cations on the basis of 24 Oxygens														
Si	5.15	5.19	5.20	5.21	5.38	5.31	5.32	5.34	5.33	5.33	5.37	5.33	5.33	5.31
Ti	0.18	0.20	0.19	0.21	0.19	0.18	0.17	0.18	0.19	0.19	0.19	0.19	0.20	0.19
Al_{tot}	3.68	3.64	3.60	3.62	3.65	3.51	3.55	3.50	3.56	3.58	3.62	3.54	3.58	3.52
Al_{IV}	4.32	4.36	4.40	4.38	4.35	4.49	4.45	4.50	4.44	4.42	4.38	4.46	4.42	4.48
Fe	2.70	2.58	2.58	2.55	2.51	2.66	2.63	2.59	2.54	2.48	2.46	2.53	2.49	2.62
Mg	2.28	2.21	2.28	2.19	2.07	2.15	2.17	2.21	2.21	2.22	2.24	2.23	2.20	2.20
Na	0.06	0.13	0.09	0.11	0.08	0.08	0.08	0.07	0.04	0.05	0.02	0.05	0.07	0.06
K	1.44	1.69	1.72	1.74	1.54	1.79	1.72	1.69	1.68	1.67	1.36	1.36	1.70	1.67
XFe	0.53	0.53	0.52	0.53	0.55	0.55	0.55	0.54	0.53	0.53	0.52	0.53	0.53	0.54
XMg	0.46	0.44	0.45	0.44	0.43	0.43	0.44	0.44	0.45	0.45	0.45	0.45	0.45	0.44

The P-T conditions of metamorphism

Baharifar (1997) estimated a temperature of 570 °C and a pressure of 430 ± 50 MPa for sillimanite-schists and garnet-staurolite-schists 340 ± 5 MPa for staurolite-schists of the study area. Sepahi et al. (2004) have estimated a temperature range of 520–560 °C for the sillimanite ± kyanite-schists using garnet-biotite thermometer. For this temperature range, they calculated a pressure of 270–350 MPa using garnet-sillimanite-plagioclase-quartz barometry. Garnet-biotite-plagioclase-muscovite-quartz and garnet-plagioclase-muscovite-quartz barometry have yielded consistent results for the same samples (~300 MPa). On the basis of field observations, metamorphic reactions, and thermobarometric calculations, maximum conditions of 250–350 MPa and 550–600 °C were suggested for the highest-grade contact metamorphic rocks (Baharifar 1997; Sepahi 1999). The peak temperature for metamorphic rocks in the migmatitic zone is estimated to be about 650–670 °C (Baharifar 2004). This estimation is in accordance with vapor-present melting at P = 300 MPa and T = 640 °C which has been suggested for Mt Stafford, Central Australia (Greenfield et al. 1998), and solidus temperature of

Table 3: Electron microprobe representative analyses (wt. %) of muscovite in migmatites (MM_1–MM_3), schists (MS_1–MS_5) and hornfelses (MH_1–MH_2) of the region.

Samples	MM_1	MM_2	MM_3	MS_1	MS_2	MS_3	MS_4	MS_5	MH_1	MH_2
SiO_2 (wt. %)	45.77	45.73	45.51	44.41	44.18	44.94	43.65	43.41	46.10	46.17
TiO_2	0.51	0.34	0.25	0.62	0.50	0.48	0.49	0.46	0.46	0.48
Al_2O_3	35.99	35.54	35.56	37.05	37.34	37.75	36.94	35.59	37.21	37.21
FeO	1.00	1.11	1.11	1.34	1.28	1.20	3.39	4.82	1.07	1.21
MnO	0.00	0.00	0.00	0.19	0.24	0.21	0.24	0.22	0.00	0.00
MgO	0.61	0.79	0.73	0.65	0.56	0.61	0.59	0.71	0.44	0.43
CaO	0.00	0.00	0.00	0.14	0.14	0.15	0.57	0.27	0.00	0.00
Na_2O	0.98	0.77	0.82	1.44	1.49	1.42	1.20	1.02	1.26	1.41
K_2O	9.68	9.76	9.80	9.26	9.13	9.01	7.77	7.64	8.84	9.12
Total	94.54	94.04	93.78	95.09	94.86	95.76	94.84	94.13	95.39	96.02
Number of cations on the basis of 24 Oxygens										
Si	6.11	6.14	6.13	5.92	5.90	5.93	5.86	5.90	6.07	6.06
Ti	0.05	0.03	0.03	0.06	0.05	0.05	0.05	0.05	0.05	0.05
Al_{tot}	5.66	5.62	5.64	5.82	5.88	5.87	5.84	5.70	5.77	5.75
Al_{IV}	2.34	2.38	2.36	2.18	2.12	2.13	2.16	2.30	2.23	2.25
Al_{VI}	3.32	3.25	3.29	3.65	3.76	–	–	–	3.55	3.51
Fe	0.11	0.12	0.13	0.15	0.14	0.13	0.38	0.55	0.12	0.13
Mg	0.12	0.16	0.15	0.13	0.11	0.12	0.12	0.14	0.09	0.08
Na	0.25	0.20	0.21	0.37	0.39	0.36	0.31	0.27	0.32	0.36
K	1.65	1.67	1.68	1.58	1.56	1.52	1.33	1.33	1.49	1.53
XFe	0.48	0.44	0.46	0.47	0.47	0.45	0.63	0.73	0.58	0.61
XMg	0.03	0.04	0.04	0.03	0.03	0.35	0.18	0.18	0.02	0.02
XAl_{vi}	0.92	0.91	0.92	0.91	0.91	–	–	–	0.93	0.93

640 °C at P = 500 MPa for the stromatic migmatites of Nelaug, Southern Norway (Gupta & Johannes 1982).

We have calculated some new P-T values using the garnet-biotite thermometry (Ferry & Spear 1978) for 3 samples from the low-grade (garnet-mica-schist from the garnet zone on Fig. 2), low–medium-grade (garnet-andalusite-schist from the andalusite zone on Fig. 2) and medium-grade rocks (garnet-sillimanite-schist from the sillimanite zone on Fig. 2). The calculated temperatures are 432, 517 and 532 °C at a pressure of 300 MPa which are consistent with field and petrographic observations.

The typical assemblage of inter-layers of cordierite-migmatites (quartz-cordierite-andalusite-biotite-K-feldspar-spinel) can be stable at a temperature higher than ~600 °C, at maximum pressure of ~300 MPa (Tinkham et al. 2001). Considering the rapid decrease in the volume of biotite in these rocks and partial replacement of andalusite porphyroblasts by cordierite-spinel symplectites in these rocks, the temperature could be higher than 650 °C but andalusite persisted metastably into the sillimanite + melt field. This is presented in the phase diagram according to White et al. (2003), with a few changes (Fig. 10) (see also Johnson et al. 2004). Sepahi (1999) considered a diapiric rise as a possible mechanism for the ascent and emplacement of the migmatites and associated S-type granites into the upper levels of crust in the region, similar to the diapiric rise of the country rocks near the Bushveld Complex in South Africa (Johnson et al. 2004).

The formation of retrograde muscovite and the second generation of staurolite (St_2) at the expense of andalusite/sillimanite porphyroblasts yields have given rise to the assemblage staurolite ± $garnet_2$ + muscovite + quartz, observed only inside and around the andalusite/sillimanite porphyroblasts close to the aplitic-pegmatitic dykes (Fig. 4). This assemblage is not stable at a pressure lower than 300 MPa and indicates higher pressure, post-migmatization conditions in the region. The following reaction could have occurred near the dykes (just incompletely) to generate such a mineral assemblage:

Andalusite/Sillimanite + Biotite + $Garnet_1$ + H_2O = Staurolite + Muscovite + $Garnet_2$ + Quartz.

A temperature of ~570 °C at ~300 MPa has been proposed for the equilibrium conditions of such a reaction (Thompson & Norton 1968; Carmichael 1970; Winkler 1974). Field observations confirm that such retrograde conditions occurred simultaneously with the intrusion of younger aplitic-pegmatitic dykes into the high-grade schists/migmatites (Fig. 5c). According to Garcia-Casco et al. (2003), staurolite in migmatites could be generated from retrograde reactions during subsequent cooling or a distinct thermal pulse. This can be supported by the occurrence of staurolite in the region around the pegmatitic-aplitic dykes cutting through the schists/migmatites of the area. This is in accordance to the latter idea.

Discussion

Possible origin(s) of the leucosome layers

Although migmatitic rocks in the Hamedan region are located near the younger porphyric granites, the degree of partial melting is not controlled by distance from the pluton contacts and is very irregular. Instead, it seems that melt fraction and migmatite type were determined by the chemical composition of parent rocks and/or by the presence of deformation/fluids in high strain zones. In the adjacent layers within an outcrop the degree of partial melting is variable, due to changes in parent rock compositions and the existence of high strain zones which enabled the movement of fluids.

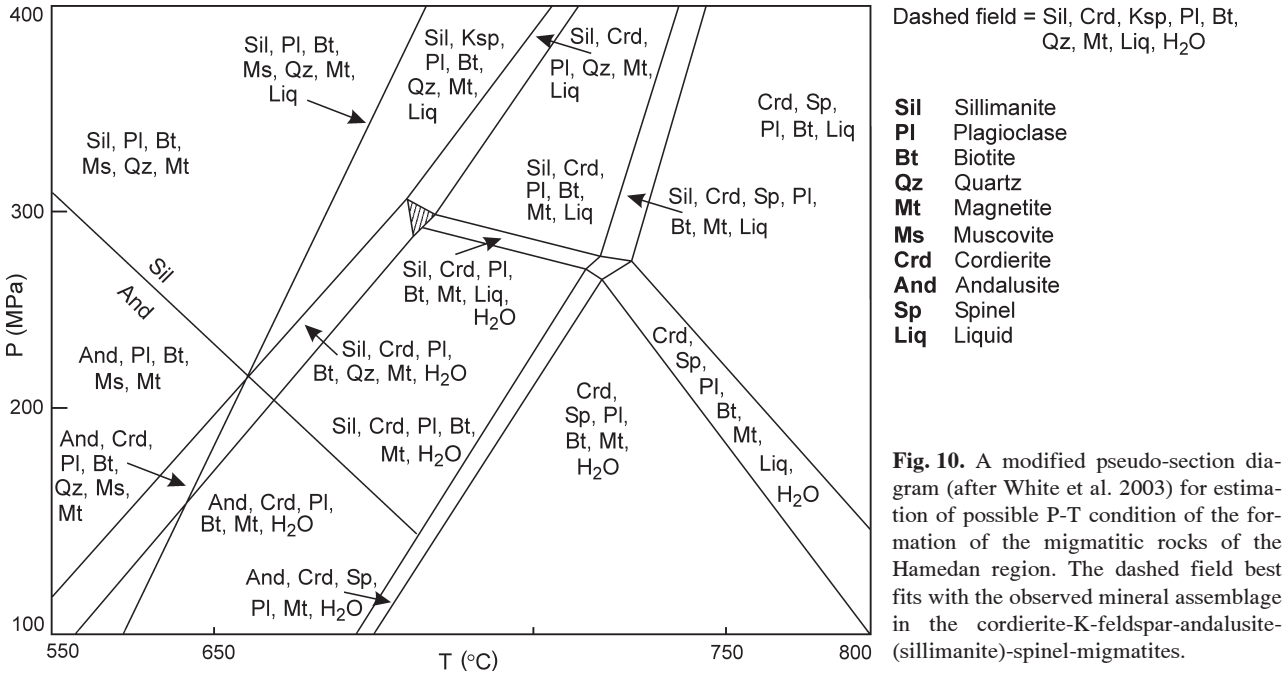

Fig. 10. A modified pseudo-section diagram (after White et al. 2003) for estimation of possible P-T condition of the formation of the migmatitic rocks of the Hamedan region. The dashed field best fits with the observed mineral assemblage in the cordierite-K-feldspar-andalusite-(sillimanite)-spinel-migmatites.

The formation of thin leucosomes, in the migmatites of the region, was possibly controlled by short-range melt movement along grain boundaries to form melt-rich layers constrained by pre-existing compositional layering (Marchildon & Brown 2003). Leucosomes in stromatic migmatites of the region are parallel to bedding planes in some parts. These layer-parallel leucosomes can be formed by sub-solidus processes and/or *in situ* melting in a closed system. Melt transfer from grain-scale sites where melting occurred to layer-parallel leucosomes was controlled by the spatial distribution of pre-existing compositional layering and foliation formed by metamorphic segregation, but some times by *in situ* partial melting (showing pinch and swell structures; Fig. 3i). Some of the leucosomes were generated by metamorphic differentiation or *in situ* partial melting showing mafic selvedges.

Accumulation of melt in the fault zones, shear zones, hinge zone of folds and boudin necks is common in the migmatitic zone of the region. Bedding and schistosity planes have also been important for the movement of melts/fluids in the parent rocks.

Partial melting occurred at a temperature near to andalusite-sillimanite univariant curve so that andalusite-, sillimanite- and andalusite-sillimanite-bearing migmatites alternate in the adjacent layers. The existence of tourmaline-rich aplites and pegmatites, and tourmalinites cutting through the medium–high-grade metamorphic rocks, and occurrence of tourmaline in the country rocks confirm a possible boron-rich environment during and after partial melting processes (e.g. Wolf & London 1997). In the boron-rich environments, the stability field of andalusite can be expanded to higher temperatures (Greenfield et al. 1998).

In the sillimanite-(andalusite)-migmatites, the size and abundance of the K-feldspar and garnet crystals commonly increase with the abundance of the leucosome portions in the migmatites. Therefore, the following reactions could have occurred simultaneously during partial melting in these rocks:

Andalusite = Sillimanite;
Biotite + Sillimanite/Andalusite + Quartz = Garnet + K-feldspar + Melt.

The higher content of garnet and K-feldspar in the migmatitic rocks (especially in leucosomes) in contrast to the lower amount of these minerals in the lower-grade equivalents of migmatites, preferred accumulation of garnet crystals in the leucosomes, univariant change of the andalusite to sillimanite in the migmatitic rocks and the absence of white mica in the medium-grade rocks of the region (except retrograde white-mica formed at the expense of some of the andalusite/sillimanite porphyroblasts), are good indicators for such reactions.

In the cordierite-migmatites the volume of leucosomes is rather higher than that in the Al_2SiO_5-bearing migmatites. There is an obvious increase in the amount of cordierite and K-feldspar in the cordierite-migmatites in contrast to the lower-grade rocks. At the same time as the increase in the abundance of cordierite and K-feldspar, the amount of biotite (and Al_2SiO_5 minerals) decreases rapidly; therefore, the following reaction may be possible during the partial melting of these rocks:

Biotite + Sillimanite/Andalusite + Quartz = Cordierite + K-feldspar + Melt.

Considering the absence of muscovite in the medium-grade rocks adjacent to the migmatites, this reaction can be more possible than a dehydration-melting reaction of muscovite. However, considering a low decrease in the amount of biotite in the Al_2SiO_5-bearing migmatites in contrast to the cordierite-bearing migmatites, an input of some fluids from the external source(s), especially in high strain zones such as shear

zones, may be necessary for the partial melting. Therefore, a complex model involving sub-solidus segregation and *in situ* partial melting assisted by H_2O (fluids) resulting from the biotite dehydration reaction may explain the observed features of migmatitic rocks in some localities. Instead, a model involving partial melting in the presence of some external fluids may better explain the features of migmatites in the shear zones.

Regional and tectonic implications

The mineral assemblages of the investigated metamorphic rocks indicate that multiple metamorphic events occurred in the Hamedan region. Some minerals such as staurolite and cordierite crystallized during two different stages of metamorphism. The mineral assemblages of migmatites comprise metastable andalusite and locally development of retrograde staurolite and muscovite ($\pm$ garnet$_2$) at the expense of Al_2SiO_5 minerals and biotite (especially near aplitic-pegmatitic dykes and post-metamorphic intrusions). The higher pressure condition of the retrograde assemblage are at odds with the isobaric conditions or decompression reactions. It is possible that aplitic-pegmatitic dykes were intruded into the environment during a higher-pressure event (collisional tectonic regime). The development of widespread late-stage quartz-kyanite veins in the region (cutting through regional and contact metamorphic rocks as well as older intrusive rocks; see also Sepahi et al. 2004) may be considered as complementary evidence for this argument.

Only in some places, migmatites occur adjacent to younger granitic bodies and they are not always common around these granitic intrusions. In many other places, they are absent in the contact zone of younger granitic intrusions, and instead hornfelsic rocks occur there. So, the major parts of the migmatites of the region are not contact migmatites. Retrograde reactions in the migmatites, adjacent to granitic bodies and aplitic-pegmatitic dykes, indicate that the intrusion of these dykes and younger granitic bodies post-date the migmatization phenomenon. This means that anatexis was not facilitated by heating from the younger granitic plutons but intrusion of older gabbroic-dioritic bodies. The occurrence of xenocrystic andalusite (partially replaced by sillimanite), in gabbro-dioritic rocks, suggests that the conditions of the regional metamorphism reached the andalusite stability field prior to the intrusion of granitic bodies into the metamorphic rocks. Contemporaneous with the gabbro-dioritic intusions, the temperature conditions reached the univariant curve between andalusite and sillimanite, and the stability field of sillimanite.

According to the evidence presented here and in the previous works, the metamorphic-magmatic history of the region can be summarized in the following stages:

1) A LP-HT arc-type metamorphism (in Jurassic-Cretaceous) involving sequential development of various index minerals including chlorite, biotite, andalusite (chiastolite), garnet (almandine-rich), staroulite (St_1), prismatic sillimanite (Sil_1), cordierite (Crd_1) and K-feldspar, development of syn-metamorphic quartz-Al_2SiO_5-bearing veins (e.g. quartz-andalusite veins and quartz-sillimanite veins (Sepahi et al. 2004; Sepahi & Cavosie 2005)) as well as the emplacement of the mafic to felsic plutonic rocks of an arc system and regional migmatization.

2) Intrusion of younger post-tectonic granitoids (i.e. the small intrusions of leucocratic granitoids). These granitic bodies generated very limited (on a meter to decimeter scale) low-grade contact metamorphism and alteration zones in the previously metamorphosed rocks and older plutonic rocks.

Acknowledgment: We are grateful of A. Berger and P. Nábelek for their review and comments on an older version of the manuscript.

References

Ahmadi-Khalaji A., Esmaeily D., Valizadeh M.V. & Rahimpour-Bonab H. 2007: Petrology and geochemistry of the granitoid complex of Boroujerd, Sanandaj-Sirjan Zone, Western Iran. *J. Asian Earth Sci.* 29, 5–6, 859–877.

Alavi M. 1994: Tectonics of Zagros orogenic belt of Iran: new data and interpretation. *Tectonophysics* 229, 211–238.

Alavi M. 2004: Regional stratigraphy of the Zagros fold-thrust belt of Iran and its proforeland evolution. *Amer. J. Sci.* 304, 1–20.

Arvin M., Pan Y., Dargahi S., Malekizadeh A. & Babaei A. 2007: Petrochemistry of the Siah-Kuh granitoid stock southwest of Kerman, Iran: Implications for initiation of Neo-Tethys subduction. *J. Asian Earth Sci.* 30, 474–479.

Ashworth J.D. 1985: Introduction. In: Ashworth J.D. (Ed.): Migmatites. *Blackie and Son*, Glasgow, 1–35.

Ashworth J.D. & McLellan E.L. 1985: Textures. In: Ashworth J.D. (Ed.): Migmatites. *Blackie and Son*, Glasgow, 180–203.

Baharifar A.A. 1997: New perspective on petrogenesis of regional metamorphic rocks of Hamedan area. *M.Sc. Thesis, Tarbiat Moallem University*, Tehran, Iran (in Farsi).

Baharifar A.A. 2004: Petrology of metamorphic rocks in the Hamedan area. *Ph.D. Thesis, Tarbiat Moallem University*, Tehran, Iran (in Farsi).

Braud J. 1987: La suture du Zagros au niveau de Kermanshah (Kurdistan Iranian): Reconstitution paleogeographique, evolution geodynamique, magmatique et structurale. *Ph.D. Thesis, Geodiffusion editeur*, Paris, France.

Brown M. 1994: The generation, segregation, ascent and emplacement of granite magma: the migmatite-to-crustally-derived granite connection in thickened orogens. *Earth Sci. Rev.* 36, 83–130.

Carmichael D.M. 1970: Intersecting isograds in the Whetstone Lake Area, Ontario. *J. Petrology* 11, 147–181.

Clarke D.B. et al. (35 co-authors) 2005: Occurrence and origin of Andalusite in peraluminous felsic igneous rocks. *J. Petrology* 46, 3, 441–472.

Ferry J.M. & Spear F.S. 1978: Experimental calibration of the partitioning of Fe and Mg between biotite and garnet. *Contr. Miner. Petrology* 66, 113–117.

Garcia-Casco A., Haissen F., Castro A., El-Hmidi H., Torres-Roldan R.F. & Millan G. 2003: Synthesis of staurolite in melting experiments of a natural metapelite: consequences for the phase relations in low-temperature pelitic migmatites. *J. Petrology* 44, 10, 1727–1757.

Greenfield J.E., Clarke G.L. & White R.W. 1998: A sequence of partial melting reactions at Mt Stafford, Central Australia. *J. Metamorph. Geol.* 16, 3, 363–378.

Gupta L.N. & Johannes W. 1982: Petrogenesis of a stromatic migmatite (Nelaug, Southern Norway). *J. Petrology* 23, 4, 548–567.

Hadipour M. 1994: Metamorphism and magmatism of Hamedan-Malayer-Teuyserkan region. *M.Sc. Thesis, Tarbiat Moallem University*, Tehran, Iran (in Farsi).

Holmquist P.J. 1921: Typen and nomenkaltur der adergesteine. *GFF* 43, 613–631.

Irani M. 1993: The study of the Alvand granitic body and its metamorphic aureole. *M.Sc. Thesis, Shahid Beheshti University*, Tehran, Iran (in Farsi).

Johnson T., Brown M., Gibson R. & Wing B. 2004: Spinel-cordierite symplectites replacing andalusite: evidence for melt-assisted diapirism in the Bushveld Complex, South Africa. *J. Metamorphic Geology* 22, 6, 529–545.

Kretz R. 1983: Symbols for rock-forming minerals. *Amer. Mineralogist* 69, 277–279.

Mahar E.M., Baker J.M., Powell R., Holland T.J.B. & Howell N. 1997: The effect of Mn on mineral stability in metapelites. *J. Metamorphic Geology* 15, 2, 223–238.

Marchildon N. & Brown M. 2002: Grain-scale melt distribution in two contact aureole rocks: implications for controls on melt localization and deformation. *J. Metamorphic Geology* 20, 4, 381–396.

Marchildon N. & Brown M. 2003: Spatial distribution of melt-bearing structures in anatectic rocks from Southern Britany, France: implications for melt transfer at grain to orogen-scale. *Tectonophysics* 364, 215–235.

Masoudi F. 1997: Contact metamorphism and pegmatite development in the region SW of Arak, Iran. *Ph.D. Thesis, Dept. Earth Sci., Univ. Leeds*, UK.

Mehnert K.R. 1968: Migmatites and the origin of granitic rocks. *Elsevier*, Amsterdam, 1–393.

Misch P. 1968: Plagioclase compositions and non-anatectic origin of migmatitic gneisses in Northern Cascade mountains of Washington State. *Contr. Mineral. Petrology* 17, 1–70.

Rashidnejad-Omran N., Emami M.H., Sabzehei M., Rastad E. & Bellon H. 2002: Lithostratigraphy and Paleozoic to Paleocene history of some metamorphic complexes from Muteh area, Sanandaj-Sirjan zone (southern Iran). *C. R. Geoscience* 334, 16, 1185–1191.

Robin Y.F. 1979: Theory of metamorphic segregation and related processes. *Geochim. Cosmochim. Acta* 43, 1587–1600.

Sadeghian M. 1994: The study of petrology of igneous and metamorphic rocks of Cheshme-Ghassaban, Hamedan. *M.Sc. Thesis, University of Tehran*, Iran (in Farsi).

Sawyer E.W. 1996: Melt segregation and magma flow in migmatites: implications for the generation of granite magmas. *Trans. Roy. Soc. Edinburgh, Earth Sci.* 87, 1–2, 85–94.

Sawyer E.W. 2001: Melt segregation in continental crust: distribution and movement of melt in anatectic rocks. *J. Metamorphic Geology* 19, 3, 291–309.

Sawyer E.W. & Barnez S.-J. 1988: Temporal and compositional differences between sub-solidus and anatectic migmatite leucosomes from the Quetio metasedimentary belt, Canada. *J. Metamorphic Geology* 6, 4, 437–450.

Sederholm J.J. 1913: Die entstehung der migmatitischen gesteine. *Geol. Rdsch.* 4, 174–185.

Sepahi A.A. 1999: Petrology of the Alvand plutonic complex with special reference on granitoids. *Ph.D. Thesis, Tarbiat Moallem Univ., Tehran*, Iran (in Farsi).

Sepahi A.A. & Athari S.F. 2006: Petrology of major granitic plutons of the northwestern part of the Sanandaj-Sirjan Metamorphic Belt, Zagros Orogen, Iran: with emphasis on A-type granitoids from the SE Saqqez area. *Neu. Jb. Mineral. Abh.* 183, 1, 93–106 (14).

Sepahi A.A. & Cavosie A. 2005: Constraints on isotope thermometry of quartz-aluminosilicate veins in the Hamedan region using Oxygen stable isotopes. *Iranian J. Crystallography and Mineralogy* 13, 2, 245–258 (in Farsi with English abstract).

Sepahi A.A., Whitey D.L. & Baharifar A.A. 2004: Petrogenesis of Andalusite-Kyanite-Sillimanite veins and host rocks, Sanandaj-Sirjan metamorphic belt, Hamedan, Iran. *J. Metamorphic Geology* 22, 2, 119–134.

Sergi A. 1997: Mafic micro-granular enclaves from the Xanthi pluton (Northern Greece): an example of mafic-felsic magma interaction. *Miner. Petrology* 61, 1–4, 97–117.

Sheikholeslami R., Bullen H., Emami M.H., Sabzehei M. & Pique A. 2003: New structural and K^{40}-Ar^{40} data for the metamorphic rocks in Neyriz area (Sanandaj-Sirjan zone, southern Iran): Their interest for an overview of the Neo-Tethyan domain in the Middle East. *C. R. Geoscience* 335, 13, 981–991.

Thomson J.B. & Norton S.A. 1968: Paleozoic regional metamorphism in New England and adjacent areas. In: Zen, E-An, et al. (Eds.): Studies of Appalachian geology: Northern and Maritime. *Inter-Science Publ. John Wiley*, New York, 319–327.

Tinkham D.K., Zuluaga C.A. & Stowell H.H. 2001: Metapelite phase equilibria in MnNCKFMASH: The effect of variable Al_2O_3 and MgO/(MgO + FeO) on mineral stability. *Geol. Material Res., Mineral. Soc. Amer.* 3, 1, 1–42.

Torkian A. 1995: The study of petrography and petrology of Alvand pegmatites (Hamedan). *M.Sc. Thesis, Univ. Tehran*, Iran (in Farsi).

Valizade M.V. & Cantagral J.M. 1975: Premieres donnees radiometriques (K-Ar et Rb-Sr) sur les micas du complexe magmatique du Mont Alvand pres Hamadan (Iran Occidental). *C. R. Hebd. Séanc. Acad. Sci., Sér. D. Sci. Natur.* 281, 1083–1086.

White R.W., Powell R. & Clarke G.L. 2003: Prograde metamorphic assemblage evolution during partial melting of metasedimentary rocks at low pressures: Migmatites from Mt Stafford, Central Australia. *J. Petrology* 44, 1937–1960.

Winkler H.G.F. 1974: Petrogenesis of metamorphic rocks. 3rd Ed. *Springer*, Berlin, 1–334.

Winkler H.G.F. 1976: Petrogenesis of metamorphic rocks. 4th Ed. *Springer*, Berlin, 1–334.

Wolf M.B. & London D. 1997: Boron in granitic magmas: stability of tourmaline in equilibrium with biotite and cordierite. *Contr. Mineral. Petrology* 130, 12–30.